GEO SOLUTIONS

220 High Street
San Luis Obispo CA 93401
805.543.8539

1021 Tama Lane, Suite 105
Santa Maria, CA 93455
805.614.6333

201 S. Milpas Street, Suite 103
Santa Barbara, CA 93103
805.966.2200

info@geosolutions.net
sbinfo@geosolutions.net

November 19, 2021
Project No. SB01549-1

Matt Cooper and Matt Goodwin
Carp Bluffs, LLC
1415 North Cahuenga Blvd
Los Angeles, California 90038

Subject: **Wave Runup and Coastal Bluff Erosion Rate**
The Farm, Carpinteria Avenue
APNs 001-170-010 and 001-170-013
Carpinteria, California

Dear Mr. Cooper and Mr. Goodwin:

1.0 INTRODUCTION

This report presents a wave runup and coastal bluff erosion rate for the proposed project "The Farm" along Carpinteria Avenue, APNs 001-170-010 and 001-170-013 in the city of Carpinteria, California (site). You have requested a site specific wave runup evaluation and bluff erosion rate for the site. This study is not an engineering geology investigation for the Site and no subsurface investigation was conducted or requested. A slope stability analysis was not requested or conducted.

2.0 SITE CONDITIONS

The site is currently utilized as a cultivation farm for agriculture and a golf practice area in the northern portion of the property. Railroad tracks traverse through the southern portion of the property. South of the railroad tracks, vacant land and open space with public access trails are present. The site maintains bluff frontage and access to the beach. Parcel 001-170-010 is approximately 4 acres in size and parcel 001-170-013 is approximately 23.3 acres. Proposed for the site are lodges, bungalows, farmland, a restaurant, various out-buildings, and open space.

The site is relatively flat with a slight slope to the south towards the coastal bluff. The top of bluff is at an approximate elevation of 70 feet. Plate 1A is a general site geologic map that depicts elevations as NAVD88 and depicts general geologic conditions. It should be understood that this study does not include a fault study and the location of the Carpinteria fault is only generally placed on Plate 1A. Plate 1B is a section line through the bluff portion of the site.

2.1 Regional Geologic Conditions

Carpinteria is located in the western portion of the Transverse Ranges geomorphic province of southern California. The Transverse Ranges province is oriented in a general east-west direction, which is transverse to the general north-northwest structural trend of the majority of California's coastal mountain

ranges. The Transverse Ranges province extends from the San Bernardino Mountains in Riverside County (east) to Point Arguello (west). The province is bounded to the north by the San Andreas and Santa Ynez faults, the east by the Mojave geomorphic province, the south by the Peninsular geomorphic province and Pacific Ocean, and the west by the Pacific Ocean.

2.2 Local Geology

Formational units were exposed along the bluff face at the site and adjacent to the site and consist of Monterey Formation shale overlain by alluvial deposits. Locally, Dibblee, 1986, maps the site as within surficial deposits (Qoa) overlying Monterey Formation units (Tm). Plate 2A is a general geologic map and Plate 2B are Geologic Explanations. The surficial deposits are an upper Pleistocene unit (last 1.8 million years before present), moderately consolidated, crudely stratified, poorly sorted sand and sandstone, gravel, conglomerate, and breccia, with rare interbeds of clay, silt, and mudstone. Boulders of up to 2-feet diameter can be seen in the bluff face. This unit forms dissected, gently south-sloping elevated terraces, interfluvial caps, and other erosional remnants as thick as 35 meters. Thickness of this unit is varies approximately 10-30 feet as observed within the bluff face at the site.

Underlying the surficial deposits is shale of the Monterey Formation. This middle to lower Miocene (11 to 23 million years before present) unit is a calcareous, siliceous, and phosphatic mudstone and shale with subordinate dolomite, porcelanite, breccia, glauconitic sandstone, and tuff (Minor et al, 2009). This unit is usually well bedded and is approximately 250 meters thick. The Monterey shale and mudstone is moderately hard to very hard with beds from 3-30 cm thick with minor to strong calcification. Some beds are massive to bioturbated. Colors are white, tan, brown, dark gray. Dolomitic concretions are found in the unit. Porcelanite is hard, brittle, and weathers light gray to white; the Monterey Formation observed in the bluff face appears generally as hard, porcelanite shale. The unit is typically folded with discontinuous faulting exhibiting small offsets. Sandstone within this unit is fine- to medium-grained with orange-tan color. Tuff within this unit weathers orange-gray to yellow-gray, with crystals of biotite and feldspar. Structural attitudes of the Monterey Formation at the bluff are depicted on Plate 1B.

A trace of the Carpinteria fault trends through the property at the site and is approximated on Plate 1A. No fault study has been conducted for this report and the exact location of the fault is not known through the site.

3.0 BLUFF RETREAT RATE

Bluff erosion and sea cliff retreat along the coast of California is generally controlled by a combination of factors including: rock type, geologic structure, soil type, bluff height, direction and magnitude of wave attack, coastline configuration, surf zone profile, amount of surface runoff over bluff tops, degree of water seepage, and other adverse man-made conditions. The effects of erosive agents acting on the bluff are greater on weaker rock types or soils.

The principal causes of sea cliff erosion and retreat along the bluff-top include the forces of natural erosion and weathering of the alluvial deposits, spalling of weathered shale, and wave attack concentrated at the base of the bluff. Static and Intrinsic sea cliff erosion are on-going active processes that act upon sea cliff bluffs. Static erosion is a process whereby a loss of soil strength is exacerbated through increased pore water within the soil. This is seen as landsliding and rock falls within a sea cliff. This process is controlled by the availability of surface and subsurface water to the face of the sea cliff. Intrinsic erosion is a process of rock and soil weathering due to chemical reaction with available water. This is the process that accounts for loosening, spalling, flaking, granulation, and pulverization of the formational units and alluvial deposits due to cycles of wet-dry, alkali-acid, and heat-cold conditions. Intrinsic weathering is the

cause of alluvial deposits or formational unit breakdown, resulting in accumulation of slope wash debris on the bluff face.

Bluff erosion and retreat are occurring at the site. Through time, the erosive power of waves and storm surge will weaken and erode the bluff, however the slopes below the railroad tracks are monitored and maintained by the Southern Pacific Railroad (and now Union Pacific Railroad). The following is a brief discussion of the factors and how they relate to the subject area.

3.1 Surficial Drainage

In the current state, surficial drainage near the top of the bluff is directed toward the top of the bluff and acts as one of the primary mechanisms for slope erosion. Accelerated rates of slope erosion will occur along the bluff as long as surficial drainage is unchecked. Surface drainage from the top of bluff should be directed to surface drainage inlets via onsite drains and pipes. Development with controlled surface drainage normally reduces the amount of erosion of the bluff.

3.2 Seismicity

The Site, like all other sites in the general area, can be affected by moderate to major earthquakes centered on one of the known large Holocene age active faults listed in Table 1. The maximum moment magnitudes are expressed, although any event on these faults could result in moderate to severe ground shaking at the subject property. Ground shaking can weaken bluff material. Material within the bluff may become dislodged and may tumble due to a seismic event. Due to the long interval between seismic events, the long-term retreat rate would not be substantially affected.

Table 1: Distance and Moment Magnitude of Closest Faults

Closest Active Faults to Site	Approximate Distance from Site to Active Fault	Moment Magnitude
Mission Ridge-Arroyo Parida	4.8	6.78
Ventura-Pitas Point	8.4	6.89
Red Mountain	2.3	7.40

The San Andreas fault is the most likely active fault to produce ground shaking at the Site although it is not expected to generate the highest ground accelerations because of its distance from the Site.

3.3 Bluff Retreat Rates

A historic bluff retreat rate for the Site based upon a historical aerial photograph evaluation was completed. Our evaluation required site-specific research, with an established rate based upon the actual data interpretation by a Certified Engineering Geologist with experience and knowledge of coastal processes and local bluff conditions.

It is recognized that there is a limit to accuracy involved in the procedure of measuring the images and comparing these to current conditions. Clarity, exact bluff location, oblique angle of measurement, and lack of features add to uncertainty in defining the bluff edge.

Surficial deposits tend to fail by slumping when they become over-weighted by precipitation during winter seasons and when there is no support from underlying formational units. Less significant erosional agents involved in bluff erosion include direct impact of precipitation on the cliff face, runoff down the cliff face, and sapping and winnowing of soils in areas of ground-water seepage.

Bluff erosion at the Site is also based upon the ability of the formational units of the Monterey Formation to resist wave attack. Storm surge coupled with large wave activity acts to weaken, dislodge, or even remove sections of the formational units. Wave energy, especially winter storm wave activity, exacerbates erosion on the bedrock.

An aerial photogrammetric investigation was conducted to determine the long-term retreat rate of the natural slope at the bluff at the site.

3.4 Retreat Rate Analysis

A January 26, 1969 aerial photograph was utilized to establish a retreat rate at the bluff at the Site. Plate 3A depicts the 1969 aerial overlain on the 2018 topographic map. "Point A" on Plate 3A is a fence corner that was observable on both the 2018 topo map and the 1969 aerial photo. This "Point A" and the railroad tracks were utilized to rectify the aerial and topographic map to a common scale. Plate 3B depicts the 1969 aerial photograph without the topographic map overlay. Plate 3C depicts the topographic map without the 1969 image. The difference between the two images is 49 years. Other older historic aerial photos were reviewed for this project but rectifying the historic aerials to the topographic map was difficult due to limited points that could be observed on the older aerials compared to points on the 2018 topographic map.

On Plate 3A, three lines were reviewed for bluff retreat. L1, L2, and L3 were measured from the railroad tracks to the bluff edge. The railroad tracks are assumed to have remained in a similar location through the years.

Line L1 was measured from the southern track to the top of the bluff on both the topographic map and the aerial photograph. L1 is 270 feet as measured from the railroad tracks to the top of bluff on the 2018 topo map. The top of bluff location along L1 on the 1969 aerial image is difficult to discern; vegetation changes due to color can be seen on the bluff edge along L1. The top of bluff on the 2018 topo map is fairly well defined but if the color change (vegetation color vs un-vegetated area {buff color}) on the 1969 aerial is used as the top of bluff, the time period between the two images would show that there is an accretion, not erosion, of bluff top (dark line of vegetation on the 1969 image {could be used as a top of bluff} is north of the 2018 current top of bluff). Line L1 does not provide sufficient evidence for a bluff erosion rate. However, this comparison does show that bluff erosion in this area of the bluff in the last 49 years has been slow due to the inability to discern differences in top of bluff erosion during the 49 year history.

Line L2 depicts a comparison of the middle portion of the bluff at the site between the 2018 topo map and the 1969 aerial. L2 is measured as 244.7 feet long. Again, the top of bluff location appears similar in both images. There is no obvious discernable difference in bluff erosion comparing the two images.

Line 3 depicts a comparison of the western portion of the bluff at the site between the 2018 image and the 1969 aerial. If the top of bluff in the 1969 aerial is taken as the change in vegetation color, there is a difference of approximately 8 feet (96 inches) of erosion between the top of bluff in the 2018 topo and the 1969 image. This point is labelled "Point B" on Plate 3A. This equates to an erosion rate of approximately 1.95 inches (rounded to 2 inches) per year for the past 49 years.

BLUFF RETREAT: 8 feet x 12 inches per foot = 96 inches = 2 inches per year
49 years 49 years

An average retreat rate of 2 inches per year was calculated for unprotected bluff at the Site. This rate can be assumed to be occurring within unprotected bluff in the vicinity of the Site.

For a period of 100-years, a 2-inch retreat rate equals 200 inches or 16.6 feet (17 feet rounded up). According to Johnsson (2003), total development setbacks should include an additional buffer, generally 10 feet, that serves to allow for uncertainty in aspects of the analysis, allows for future increase in bluff retreat due to sea level rise, and assures that at the end of the design life of the structure that the foundation is not being undermined.

With the addition of the 10-foot buffer, the total setback for development can be assumed to be 27 feet from the current top of bluff.

The 27 foot setback is demarcated on Plate 1B. It should be noted that the assumed bluff retreat rates are considered an average, whereas in nature, erosional processes are often episodic and irregular. Short-term (yearly) bluff retreat rates may vary significantly from the long-term average due to storm activity or seismic events.

4.0 WAVE RUNUP ANALYSIS

4.1 Sea Level Rise

To incorporate the changes in sea level rise anticipated to occur of the next 100 years, the State of California Sea-Level Rise Guidance (2018 update) was utilized. Table 22 on p.66 of this document (a portion of this document in contained within this letter) shows Santa Barbara having a 2.4-foot sea-level rise by the year 2120 with a probability of 53% with a high emission category (for year 2100). Higher sea-level rise in that year have a lower probability. A probabilistic projection on Table 24 shows that the likely range of sea level rise at 66% probability is between 4.8 mm to 15mm per year. For 100 years, the middle of this range is 10mm per year which is 3.28 feet. For this study, a sea level rise of 3.28 feet is used in this analysis.

4.2 100-year Design Stillwater Elevation

The design water level in this analysis is the maximum Stillwater level under a typical 100-year recurrence condition. Water level is dependent upon several factors including tide, storm surge, wind set up, inverse barometer, and climatic events (El Nino). For this study, the maximum highest observed water level in the area was on 12/13/2012 with a highest tide of 10.79 feet. This data is relative to NAVD88 as published by NOAA datums for 9411340, Santa Barbara (see graph at end of report).

Based upon the highest tide information, the 100-year design Stillwater elevation in NAVD 88 datum would be as follows:

100-year design Stillwater elevation = 10.79 feet (highest water level observed, 2012) + 3.28 feet (sea level change) = 14.07 feet (NAVD 88).

4.3 100-year Design Stillwater Depth (Ds)

To establish the 100-year Design Stillwater Depth (Ds) along the shoreline, the maximum scour depth must first be determined. At the subject site, sand is present at the base of the bluff but also bedrock is exposed. It is estimated that winter scour depth of 0 feet of sand could occur at the site due to the presence of bedrock maintaining a base that waves would scour. This is reasonable due to the visual observation of bedrock exposed at the base of the bluff. The elevation at the base of the bluff at the site is approximately 8 feet. Due to the scour depth being 0 (zero), no scour depth was subtracted from the Stillwater depth. Therefore the design Stillwater depth (100-year design Stillwater elevation {14.07 feet}) minus scour depth elevation {0 feet} along the bluff is equal to 14.07 (Ds).

4.4 100-year Maximum Breaking Wave Height (Hb)

Data regarding storms along the Southern California coast during the winter of 1982-1983 (Denison and Robertson, 1985) were used as a guideline for determining the maximum breaking wave height at the site. These storms data are considered to be comparable to the 100-year storm events. In January, 1983, wave heights from 6 to 15 feet with 4-6-second periods were recorded; these waves were considered to be the most severe of that winter. For this analysis, the breaking wave height used was 15 feet with a 6-second period (Hb = 15 feet). During a storm event similar to those experienced in 1982-1983, the wave would likely break offshore and run up along the scoured beach surface. The beach surface slope is calculated from beach length vs beach height; beach length varies due to exposed bedrock and areas of no exposed bedrock (sand). An average slope of beach is calculated as a rise of 2 feet in a length of 20 feet giving a beach slope of 5.7 degrees.

4.5 100-Year Wave Runup Elevation (R)

Wave run-up is the vertical height above the Stillwater level to which a sea wave will rise up on a broad beach, a bluff face, or a bluff protection structure. At the subject site, the wave run-up elevation is estimated at the beach at the base of the bluff. Determination of wave run-up height was based upon the Naval Facilities Engineering Command manual (see attached Figure 7-11 at end of this report, NAVFAC, 1982), a 15 foot breaking wave height, and a 6-second period (t), a scoured beach surface of 0 feet below the existing beach surface (elevation of 8 feet), and a beach slope angle of 5.7 degrees.

$R = Hb \times R/Hb$

$Ds/Hb = 14.07/15 = 0.938$; therefore Figure 7-11 was used to get R/Hb

$Hb/gt^2 = 15/32.2(6)^2 = 0.0129$

R/Hb = (from graph) 0.62

R = Hb (15 feet) x 0.62 = 9.3 feet

Where R = wave runup in feet, Hb is height of breaking wave in feet, Ds is design Stillwater depth, t is time, g is gravity.

The addition of the 100-year wave run-up height of 9.3 feet to the 100-year stillwater elevation of 10.79 feet plus the addition of sea level rise of 3.28 feet yields a total 100-year wave run-up elevation with sea level rise equals 23.37 feet (NAVD88). The current top of bluff is approximately 70-feet (NAVD88) with a beach height currently at approximately 8-feet (NAVD88).

4.6 Tsunamis

The State of California has updated (2021) California Tsunami Hazard Area maps (State of California, 2021) for the community of Carpinteria. These maps are "to assist cities and counties in identifying their tsunami hazard for tsunami response planning. This map, and the information presented herein, is not a legal document and does not meet disclosure requirements for real estate transactions nor for any other regulatory purpose." Plate 4 depicts the local Tsunami Hazard Map which depicts a yellow zone or, a "tsunami hazard area" as up to approximately the rail road tracks at the site.

Hazardous tsunamis along the California coast are generally associated with seismic events and are typically caused by vertical displacement of submarine faults. For the Santa Barbara Channel, the Channel Islands Thrust (CIT) is a north dipping blind trust fault that is responsible for uplift of the Channel Islands south of Santa Barbara coast. Maximum surface-wave fault magnitudes and coseismic displacement were used to estimate a tsunami runup of 2 meters (6.5 feet) along the Santa Barbara coast (Borrero et al, 2000).

Tsunami waves originating from distant earthquakes on the coast of Japan, Alaska, and Hawaii have historically only produced a few feet of rise above mean high tide (Lander et al, 1993). The seismic event that occurred in Japan on March 11, 2011 produced an 8.9 magnitude earthquake. News reports indicated that this earthquake caused a tsunami tidal surge into Morro Bay, California that was documented as one of the highest surges recorded along the California Coast. The highest surge was documented at about 5 feet (tide height was at approximately 1 foot at time of recording and went almost to 6 feet in height). This report utilizes a 2 meter (6.5 feet) tsunami height as additive to the wave runup.

Therefore, the maximum 6.5-foot estimated tsunami surge was added to the 100-year design wave runup elevation of 23.37 feet to obtain a maximum tsunami flood elevation of 29.87 feet (NAVD88). This elevation is plotted on section line A-A', Plate 1B.

As the top of bluff is at approximate elevation of 70 feet NAVD88, it is our opinion that there is a low potential for flooding to reach the top of bluff as a result of a 100-year storm event or from a tsunami occurring during a 100-year storm event.

5.0 CONCLUSION

5.1 Bluff Retreat

An average retreat rate of 2 inches per year was calculated for unprotected bluff at the Site. For a period of 100-years, a 2-inch retreat rate equals 200 inches or 16.6 feet (17 feet rounded up). According to Johnsson (2003), total development setbacks should include an additional buffer, generally 10 feet, that serves to allow for uncertainty in aspects of the analysis, allows for future increase in bluff retreat due to sea level rise, and assures that at the end of the design life of the structure that the foundation is not being undermined. **With the addition of the 10-foot buffer, the total setback for development can be assumed to be 27 feet from the current top of bluff for a period of 100-years.**

5.2 Wave Runup

Wave run-up is the vertical height above the Stillwater level to which a sea wave will rise up on a broad beach, a bluff face, or a bluff protection structure. At the subject site, the wave run-up elevation is estimated at the beach at the base of the bluff. The addition of the 100-year wave run-up height of 9.3 feet to the 100-year stillwater elevation of 10.79 feet plus the addition of sea level rise of 3.28 feet yields **a total 100-year wave run-up elevation with sea level rise equals 23.37 feet (NAVD88)**. With the

addition of a potential 6.5 foot tsunami surge, the maximum tsunami flood elevation is 29.87 feet. The current top of bluff is approximately 70-feet (NAVD88) with a beach height currently at approximately 8-feet (NAVD88). **With the addition of a tsunami surge of 6.5 feet to the 100-year design wave runup elevation of 23.37 feet, a maximum tsunami flood-wave runup elevation of 29.87 feet (NAVD88) has been calculated for the bluff at the site.**

If you have any questions or require additional assistance, please contact the undersigned at (805) 543-8539.

Sincerely,
GeoSolutions, Inc.

John Kammer, Principal
Certified Engineering Geologist #2118
Certified Hydrogeologist #502

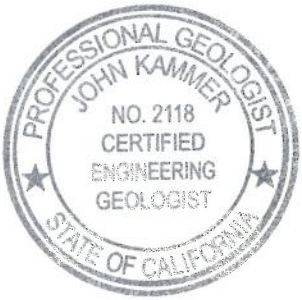

V:\SB01500-SB01999\SB01549-1 carp bluffs The Farm\Geology\sb01549-1 The Farm wave runup.docx

REFERENCES

Borrero, Jose C., Dolan, James F., and Synolakis, Costas E., 2000, American Geophysical Union, University of Southern California, Tsunamis Within the Eastern Santa Barbara Channel. Vol. 0, No. 0.

California Emergency Management Agency, California Geological Survey, University of Southern California, January 31, 2009, Tsunami Inundation Map for Emergency Planning, Carpinteria Quadrangle, State of California, County of Santa Barbara.

Cheryl Hapke, Dave Reid, 2007, The National Assessment of Shoreline Change Part 4, Historical Coastal Cliff Retreat along the California Coast, USGS, Open File Report 2007-1122.

Cheryl Hapke, Dave Reid, Bruce Richmond, Peter Ruggiero and Jeff List, 2006, The National Assessment of Shoreline Change Part 3, Historical Shoreline Change and Associated Coastal Land Loss Along Sandy Shorelines of the California Coast, USGS, Open File Report 2006-1219.

Denison, F.E. and Robertson, H.S., 1985, September. "1982-1983 Winter Storms Damage, Malibu Coastline," in California Geology.

Dibblee, Thomas W., 1986, Geologic Map of the Carpinteria Quadrangle, Santa Barbara County, California. Map #DF-04.

Griggs, Gary; Patsch, Kiki; and Savoy, Lauret, 2005, Living with the Changing California Coast, University of California Press.

Johnsson, Mark J., 2003, Establishing Development Setbacks from Coastal Bluffs, *in* Magoon, Orville et al. (eds) Proceedings, California and the World Ocean '02. Reston, Virginia: American Society of Civil Engineers.

Lander, J.F., P.A. Lockridge, M.J. Kozuch, 1993, "Tsunamis Affecting the West Coast of the United States 1806-1992." NGDC Key to Geophysical Records Documentation No. 29.

Minor, Scott A., Kellogg, Karl S., Stanley, Richard G., Stone, Paul, Powell, Charles L., Gurrola, Larry D., Selting, Amy J., 2009. Geologic Map of the Santa Barbara Coastal Plain Area, Santa Barbara County, California, United States Geological Survey.

NAVFAC (Naval Facilities Engineering Command), April, 1982. Coastal Protection Design Manual, 26.2, U.S. Navy.

State of California Sea-Level Rise Guidance, 2018 update. California Natural Resources Agency and California Ocean Protection Council. Appendix 3.

State of California, 2021, Tsunami Hazard Area Map, Carpinteria, Santa Barbara County, produced by the California Geological Survey, the California Governor's Office of Emergency Services, and AECOM.

University California Santa Barbara, Map and Imagery Lab, Aerial photograph dated 1-26-1969.

Waters Cardenas, Alta Land Title Survey, 4-27-2018, Tract "H". Topographic map of site.

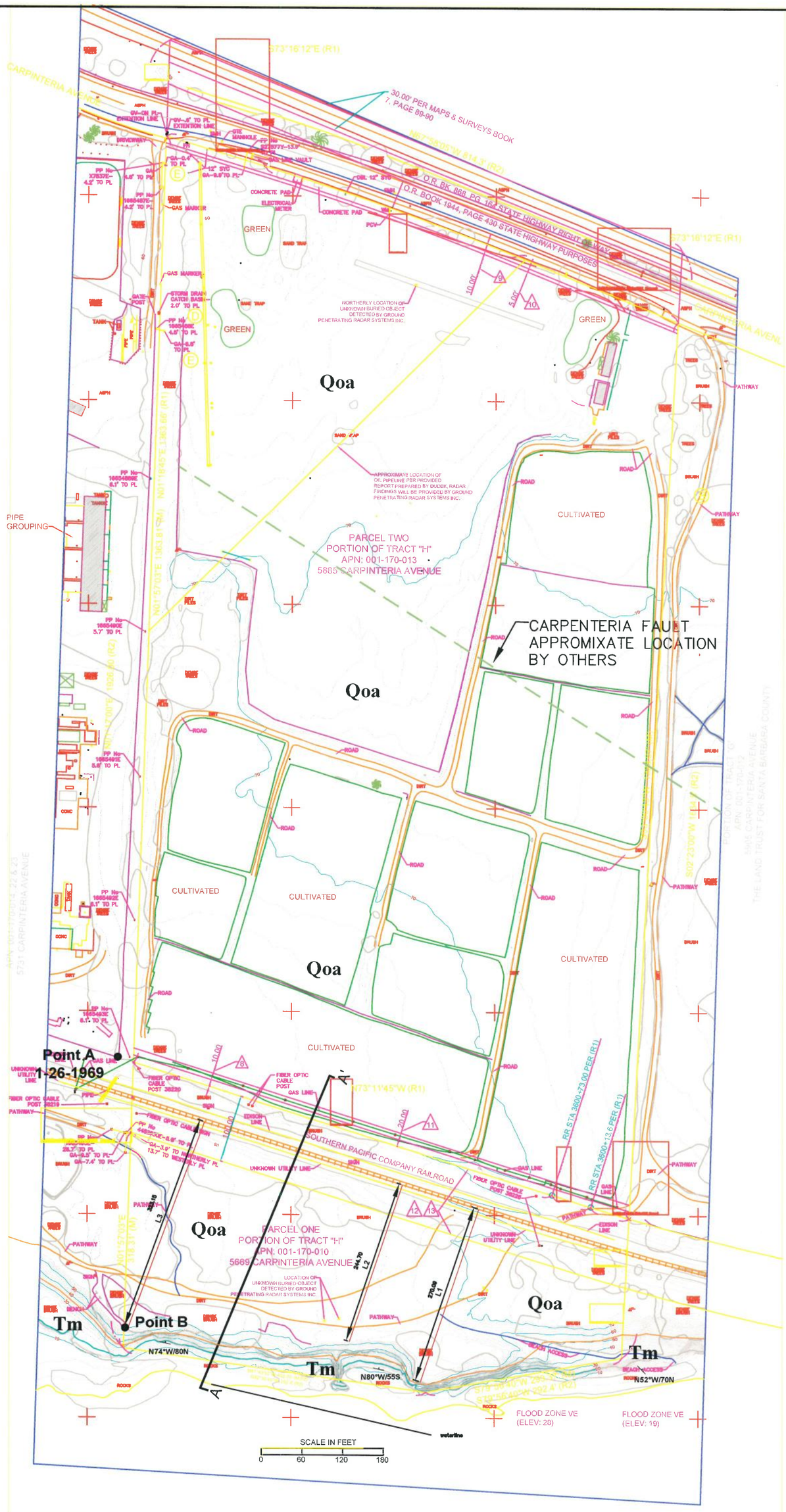

GeoSolutions, Inc.
201 S Milpas Street, Unit 103
Santa Barbara, CA 93103
(805) 966-2200

SITE GEOLOGY MAP

THE FARM, CARPINTERIA AVENUE
CARPINTERIA AREA, SANTA BARBARA COUNTY, CALIFORNIA

PLATE
1A

PROJECT
SB01549-1

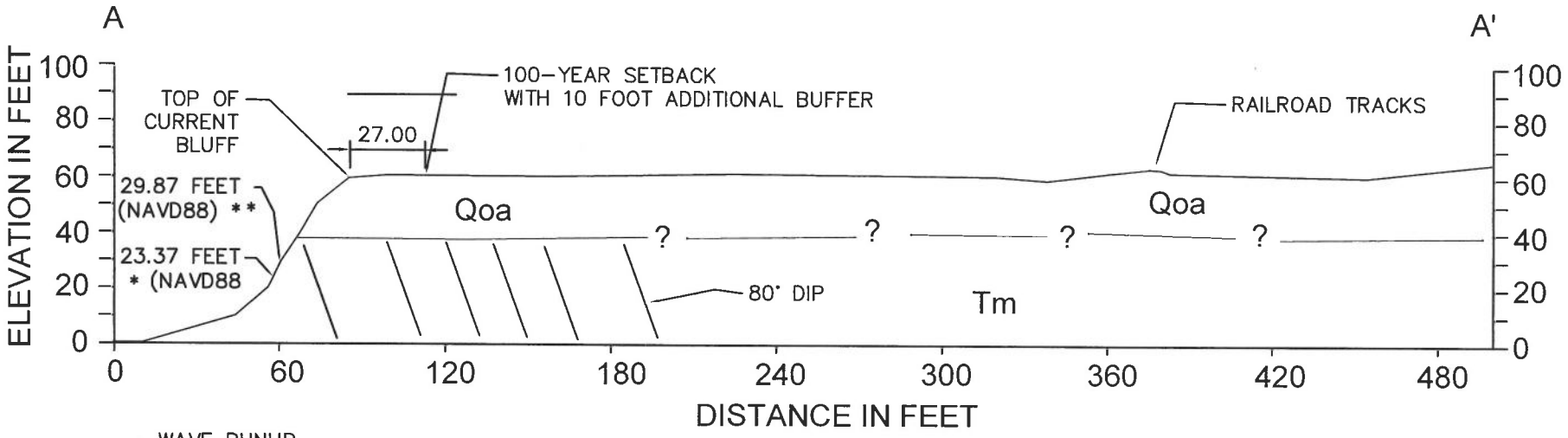

* WAVE RUNUP

* * WAVE RUNUP WITH ADDITION OF TSUNAMI SURGE

LEGEND

—— ? —— Contact - ? where approximate

Qoa - Older Alluvium

Tm - Monterey Formation

GeoSolutions, Inc.
201 S Milpas Street, Unit 103
Santa Barbara, CA 93103
(805) 966-2200

SITE CROSS SECTION

THE FARM, CARPINTRIA AVENUE
CARPINTERIA AREA, SANTA BARBARA COUNTY, CALIFORNIA

PLATE
1B

PROJECT
SB01549-1

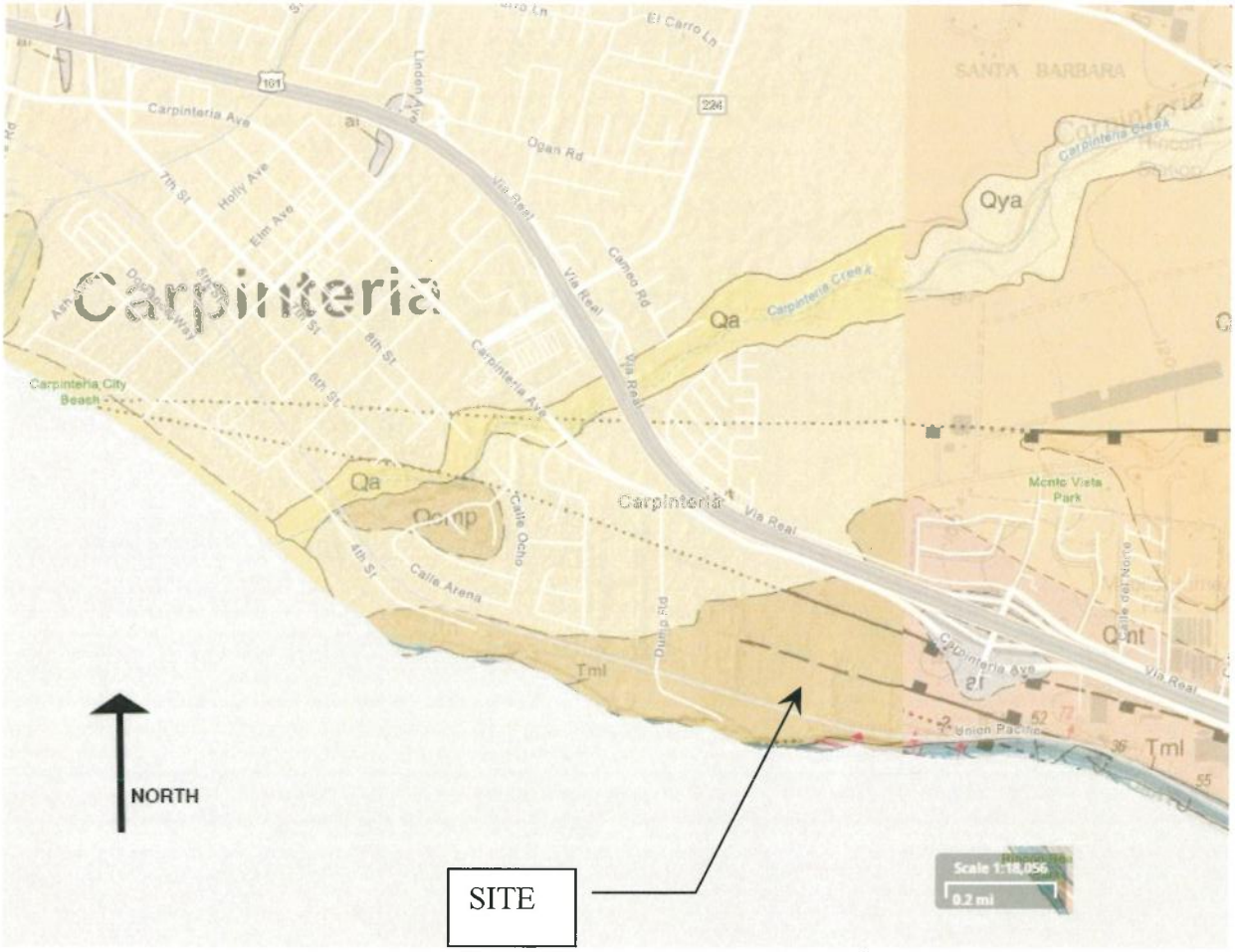

GeoSolutions, Inc.
201 S Milpas Street, Unit 103
Santa Barbara, CA 93103
(805) 966-2200

SITE GEOLOGIC MAP

Dibble, 1986
THE FARM, CARPENTRIA AREA
SANTA BARBARA COUNTY, CALIFORNIA

PLATE
2A

PROJECT NO:
SB01549-1

CARPINTERIA MAP (DF-04)
LEGEND

SURFICIAL SEDIMENTS

Qe *Beach sand deposits*
Qg *Stream channel deposits, mostly gravel and sand*
Qa *Alluvium: unconsolidated floodplain deposits of silt, sand and gravel*

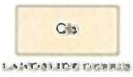

LANDSLIDE DEBRIS

OLDER DISSECTED SURFICIAL SEDIMENTS

Qos *Former alluvial deposits of silt, sand and gravel, in places weakly consolidated; local unconformities at base*
Qog *Cobble-bouldler fan gravel and conglomerate deposits composed largely of sandstone detritus*

— UNCONFORMITY —

CASITAS FORMATION

Nonmarine; early to middle (?) Pleistocene age

Qca *Weakly consolidated alluvial deposits: gray to tan cobble-boulder gravel and gray to reddish sand and clay*

— UNCONFORMITY —

MONTEREY SHALE

Marine; early to late Miocene age

Tm *Upper shale unit: white-weathering, thin bedded, hard, platy to brittle siliceous shale; Mohnian Stage*
Tml *Lower shale unit: white weathering, soft, flasle to punky clay shale with interbeds of hard siliceous shale and thin limestone strata; lower Mohnian to uppermost Saucesian Stages*

Holocene
Pleistocene
QUATERNARY

GEOLOGIC SYMBOLS

not all symbols shown on each map

FORMATION CONTACT *dashed where inferred or indefinite, dotted where concealed*

MEMBER CONTACT *between units of a formation* ..... Prominent bed

CONTACT BETWEEN SURFICIAL SEDIMENTS *located only approximately in places*

FAULT: *Dashed where indefinite or inferred, dotted where concealed, queried where existance is doubtful. Parallel arrows indicate inferred relative lateral movement. Relative vertical movement is shown by U/D (U=upthrown side, D=downthrown side). Short arrow indicates dip of fault plane. Sawteeth are on upper plate of low angle thrust fault.*

FOLDS: *overturned* ANTICLINE SYNCLINE

arrow on axial trace of fold indicates direction of plunge; dotted where concealed by surficial sediments

Strike and dip of sedimentary rocks

inclined | *inclined (approximate)* | *overturned* | *horizontal* | *vertical*

Strike and dip of metamorphic or igneous rock foliation or flow banding or compositional layers

inclined | *inclined (approximate)* | *vertical* | *overturned*

OTHER SYMBOLS:

Direction of landslide movement | *Outline of water bodies shown on map* | *water well* | *oil well* | *springs*

GeoSolutions, Inc.
201 S Milpas Street, Unit 103
Santa Barbara, CA 93103
(805) 966-2200

GEOLOGIC EXPLANATIONS

Dibble, 1986
THE FARM, CARPENTRIA AREA
SANTA BARBARA COUNTY, CALIFORNIA

PLATE
2B

PROJECT NO:
SB01549-1

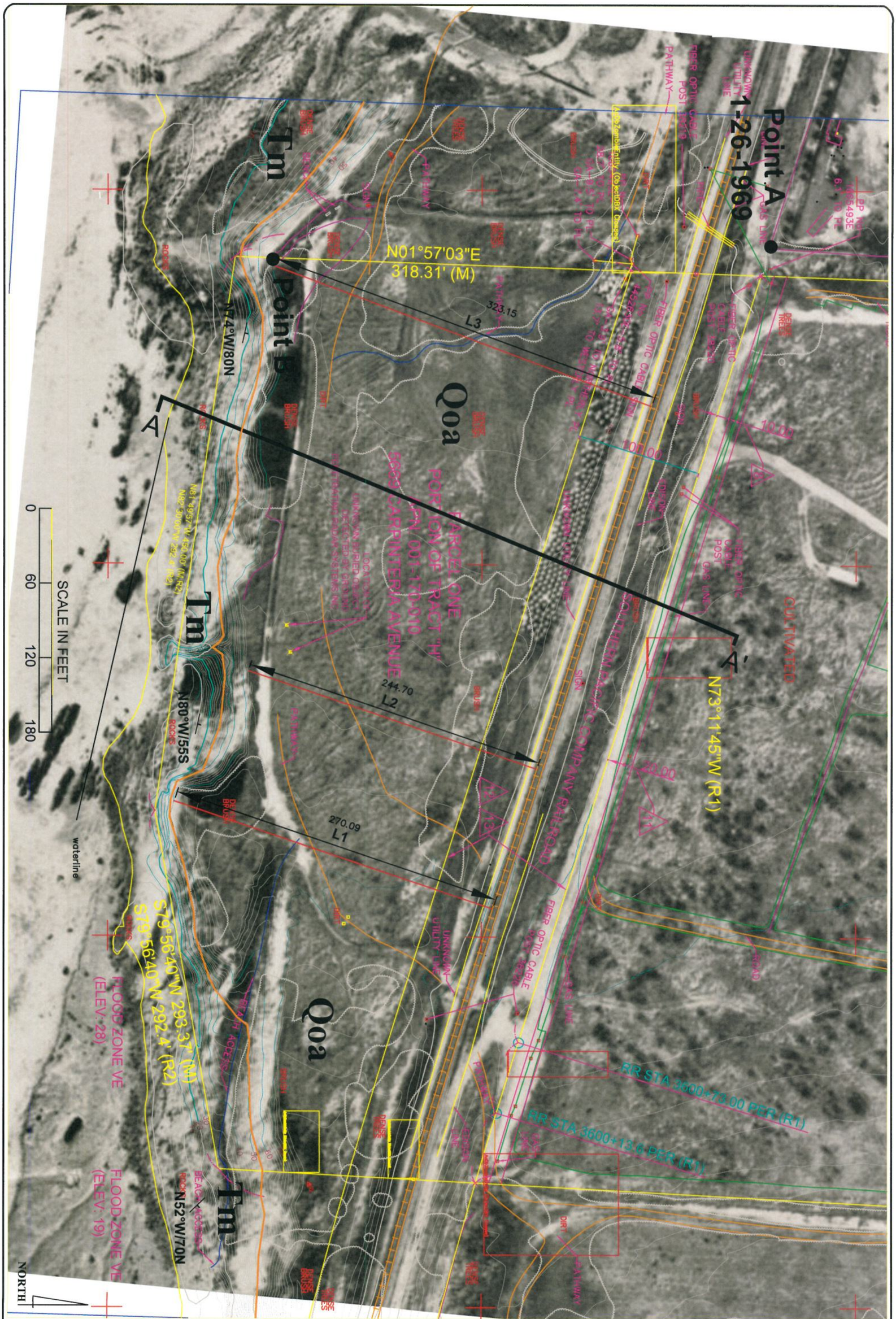

GeoSolutions, Inc.
201 S Milpas Street, Unit 103
Santa Barbara, CA 93103
(805) 966-2200

1/26/1969 AERIAL WITH TOPO OVERLAY 4/27/2018

THE FARM, CARPINTERIA AVENUE
CARPINTERIA AREA, SANTA BARBARA COUNTY, CALIFORNIA

PLATE
3A

PROJECT
SB01549-1

GeoSolutions, Inc.
201 S Milpas Street, Unit 103
Santa Barbara, CA 93103
(805) 966-2200

1969 AERIAL PHOTOGRAPH

THE FARM, CARPINTERIA AVENUE
CARPINTERIA AREA, SANTA BARBARA COUNTY, CALIFORNIA

PLATE
3B

PROJECT
SB01549-1

SITE TOPO OVERLAY 4/27/2018

THE FARM, CARPINTERIA AVENUE

CARPINTERIA AREA, SANTA BARBARA COUNTY, CALIFORNIA

PLATE 3C

PROJECT SB01549-1

Point A
1-26-1969

Point B

A

A'

PARCEL ONE
PORTION OF TRACT "H"
APN: 001-170-010
5669 CARPINTERIA AVENUE

CULTIVATED

SOUTHERN PACIFIC COMPANY RAILROAD

N73°11'45"W (R1)

RR STA 3600+73.00 PER (R1)

RR STA 3600+13.6 PER (R1)

N01°57'03"E 318.31' (M)

323.15 L3

244.70 L2

270.09 L1

N74°W/80N

N80°W/55S

N52°W/70N

S79°56'40"W 293.37' (M)

S79°56'40"W 292.4' (R2)

N81°49'57"W 460.00' (M,R2)

N82°30'00"W 292.4' (R2)

LOCATION OF UNKNOWN BURIED OBJECT DETECTED BY GROUND PENETRATING RADAR SYSTEMS INC.

PP No 1665493E 6.1' TO PL

PP No 1665493E 28.7' TO PL

GA-9.5' TO PL

GA-7.4' TO PL

PP No 4452630E-5.8' TO PL

GA-3.9' TO NORTHERLY PL

13.7' TO WESTERLY PL

FIBER OPTIC CABLE POST 38220

FIBER OPTIC CABLE POST 38219

FIBER OPTIC CABLE POST

FIBER OPTIC CABLE SIGN

FIBER OPTIC CABLE POST 38226

UNKNOWN UTILITY LINE

GAS LINE

EDISON LINE

PIPE

PATHWAY

DIRT

BRUSH

SIGN

DENSE TREES

DENSE BRUSH

BENCH

ROCKS

BEACH ACCESS

ROAD

10.00

20.00

100.00

FLOOD ZONE VE (ELEV: 28)

FLOOD ZONE VE (ELEV: 19)

Qoa

Tm

waterline

SCALE IN FEET

0 60 120 180

NORTH

GeoSolutions, Inc.
201 S Milpas Street, Unit 103
Santa Barbara, CA 93103
(805) 966-2200

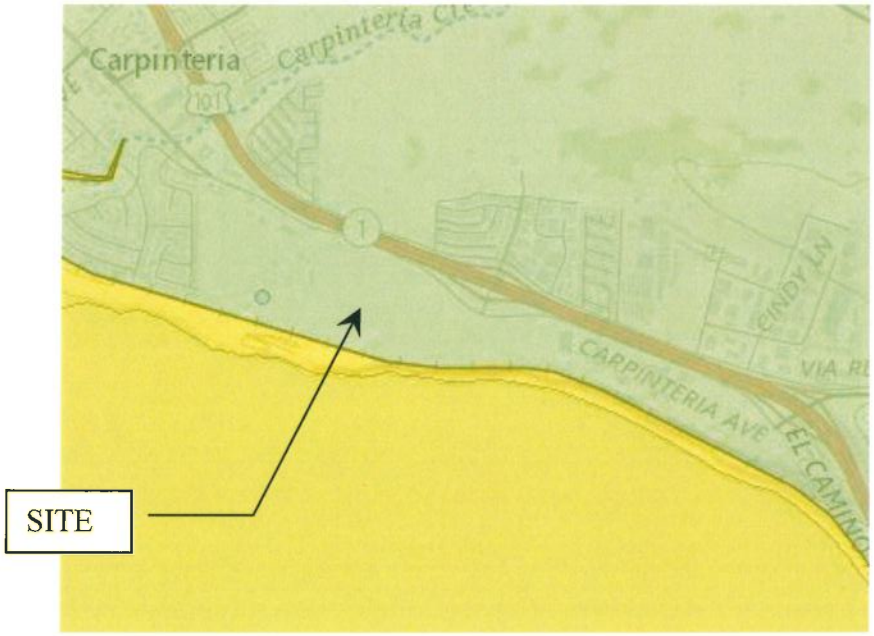

GeoSolutions, Inc.
201 S Milpas Street, Unit 103
Santa Barbara, CA 93103
(805) 966-2200

Tsunami Hazard Area Map

THE FARM, CARPENTERIA AREA
SANTA BARBARA COUNTY, CALIFORNIA

PLATE
4

PROJECT NO:
SB01549-1

State of California Sea-Level Rise Guidance

2018 UPDATE

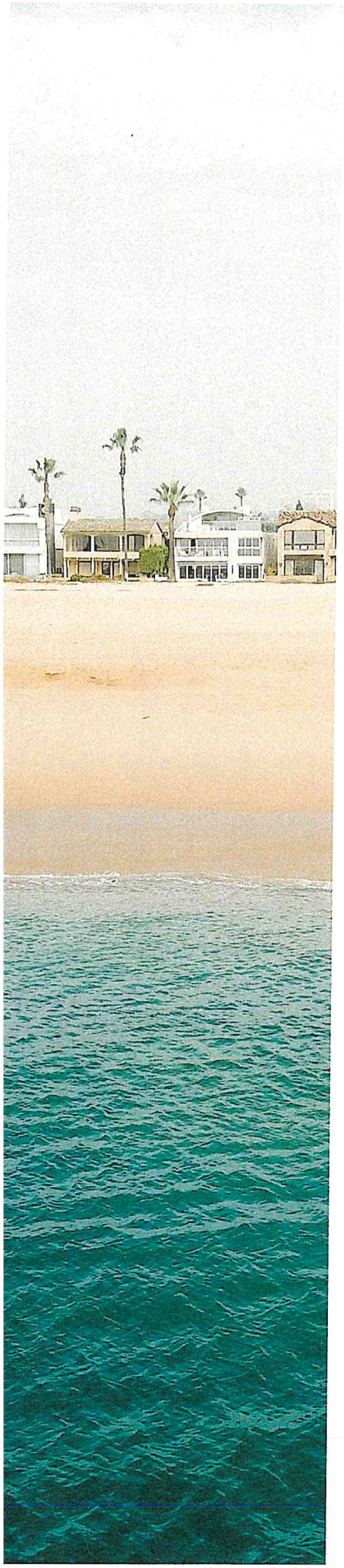

Table of Contents

CALIFORNIA natural resources AGENCY

CALIFORNIA OCEAN PROTECTION COUNCIL

TABLE 22: Projected Sea-Level Rise (in feet) for Santa Barbara

Probabilistic projections for the height of sea-level rise shown below, along with the H++ scenario (depicted in blue in the far right column), as seen in the Rising Seas Report. The H++ projection is a single scenario and does not have an associated likelihood of occurrence as do the probabilistic projections. Probabilistic projections are with respect to a baseline of the year 2000, or more specifically the average relative sea level over 1991 - 2009. High emissions represents RCP 8.5; low emissions represents RCP 2.6. ***Recommended projections for use in low, medium-high and extreme risk aversion decisions are outlined in blue boxes below.***

		Probabilistic Projections (in feet) (based on Kopp et al. 2014)					*H++ scenario (Sweet et al. 2017) †Single scenario*
		MEDIAN	LIKELY RANGE		1-IN-20 CHANCE	1-IN-200 CHANCE	
		50% probability sea-level rise meets or exceeds...	*66% probability sea-level rise is between...*		*5% probability sea-level rise meets or exceeds...*	*0.5% probability sea-level rise meets or exceeds...*	
				Low Risk Aversion		**Medium - High Risk Aversion**	**Extreme Risk Aversion**
High emissions	2030	0.3	0.2 -	0.4	0.5	0.7	1.0
	2040	0.5	0.3 -	0.7	0.8	1.1	1.6
	2050	0.7	0.4 -	1.0	1.2	1.8	2.5
Low emissions	2060	0.7	0.4 -	1.0	1.4	2.2	
High emissions	2060	0.9	0.6 -	1.3	1.6	2.5	3.6
Low emissions	2070	0.9	0.5 -	1.3	1.7	2.8	
High emissions	2070	1.1	0.7 -	1.7	2.1	3.3	4.9
Low emissions	2080	1.0	0.5 -	1.5	2.0	3.6	
High emissions	2080	1.4	0.9 -	2.1	2.7	4.3	6.3
Low emissions	2090	1.1	0.6 -	1.8	2.4	4.4	
High emissions	2090	1.7	1.1 -	2.6	3.3	5.3	7.9
Low emissions	2100	1.2	0.6 -	2.0	2.9	5.3	
High emissions	2100	2.1	1.2 -	3.1	4.1	6.6	9.8
Low emissions	2110*	1.3	0.7 -	2.1	3.0	5.9	
High emissions	2110*	2.2	1.4 -	3.2	4.2	6.9	11.5
Low emissions	2120	1.4	0.7 -	2.4	3.5	7.0	
High emissions	2120	2.5	1.7 -	3.7	4.9	8.2	13.7
Low emissions	2130	1.5	0.8 -	2.6	3.9	8.0	
High emissions	2130	2.9	1.8 -	4.2	5.6	9.5	16.0
Low emissions	2140	1.6	0.8 -	2.9	4.4	9.1	
High emissions	2140	3.1	2.0 -	4.8	6.4	11.0	18.6
Low emissions	2150	1.8	0.7 -	3.2	5.0	10.5	
High emissions	2150	3.5	2.2 -	5.3	7.2	12.6	21.4

**Most of the available climate model experiments do not extend beyond 2100. The resulting reduction in model availability causes a small dip in projections between 2100 and 2110, as well as a shift in uncertainty estimates (see Kopp et al. 2014). Use of 2110 projections should be done with caution and with acknowledgement of increased uncertainty around these projections.*

TABLE 23: Probability that Sea-Level Rise will meet or exceed a particular height (in feet) in Santa Barbara

Estimated probabilities that sea-level rise will meet or exceed a particular height are based on Kopp et al. 2014. All heights are with respect to a 1991 – 2009 baseline; values refer to a 19-year average centered on the specified year. Areas shaded in grey have less than a 0.1% probability of occurrence. Values below are based on probabilistic projections; for low emissions (RCP 2.6) the starting year is 2060 as we are currently on a high emissions (RCP 8.5) trajectory through 2050; ***the H++ scenario is not included in this table.***

SANTA BARBARA - High emissions (RCP 8.5)

	Probability that sea-level rise will meet or exceed... (excludes H++)									
	1 FT.	2 FT.	3 FT.	4 FT.	5 FT.	6 FT.	7 FT.	8 FT.	9 FT.	10 FT.
2030										
2040	1.3%									
2050	14%	0.2%								
2060	40%	2%	0.2%							
2070	64%	7%	0.8%	0.2%	0.1%					
2080	78%	20%	3%	0.7%	0.2%	0.1%	0.1%			
2090	86%	37%	8%	2%	0.7%	0.3%	0.1%	0.1%	0.1%	
2100	89%	53%	19%	6%	2%	1%	0.3%	0.2%	0.1%	0.1%
2150	98%	87%	63%	38%	20%	11%	6%	3%	2%	1%

SANTA BARBARA - Low emissions (RCP 2.6)

	Probability that sea-level rise will meet or exceed... (excludes H++)									
	1 FT.	2 FT.	3 FT.	4 FT.	5 FT.	6 FT.	7 FT.	8 FT.	9 FT.	10 FT.
2060	21%	0.8%	0.1%							
2070	35%	2%	0.3%	0.1%						
2080	48%	6%	1%	0.3%	0.1%	0.1%				
2090	57%	11%	2%	0.7%	0.3%	0.2%	0.1%	0.1%		
2100	63%	17%	4%	1%	0.6%	0.3%	0.2%	0.1%	0.1%	
2150	76%	42%	19%	9%	5%	3%	2%	1%	1%	1%

TABLE 24: Projected Average Rate of Sea-Level Rise (mm/year) for Santa Barbara

Probabilistic projections for the rates of sea-level rise shown below, along with the H++ scenario (depicted in blue in the far right column.) Values are presented in this table as mm/yr, as opposed to feet as in the previous two tables, to avoid reporting values in fractions of an inch. The H++ projection is a single scenario and does not have an associated likelihood of occurrence as do the probabilistic projections. Probabilistic projections are with respect to a baseline of the year 2000, or more specifically the average relative sea level over 1991 - 2009. High emissions represents RCP 8.5; low emissions represents RCP 2.6. For low emissions (RCP 2.6) the starting year is 2060 as we are currently on a high emissions (RCP 8.5) trajectory through 2050.

		Probabilistic Projections (mm/yr) (based on Kopp et al. 2014)				H++ scenario (Sweet et al. 2017) *Single scenario
		MEDIAN	LIKELY RANGE	1-IN-20 CHANCE	1-IN-200 CHANCE	
		50% probability sea-level rise meets or exceeds...	*66% probability sea-level rise is between...*	*5% probability sea-level rise meets or exceeds...*	*0.5% probability sea-level rise meets or exceeds...*	
High emissions	2030 - 2050	5.6	3.3 - 8.2	11	16	24
Low emissions	2060 - 2080	4.1	1.9 - 7.0	10	21	
High emissions	2060 - 2080	8.3	5.1 - 12	16	27	41
Low emissions	2080 - 2100	3.9	0.91 - 7.8	12	27	
High emissions	2080 - 2100	9.4	4.8 - 15	21	36	53

Datums for 9411340, Santa Barbara CA

NOTICE: All data values are relative to the NAVD88.

Elevations on NAVD88

Station: 9411340, Santa Barbara, CA
Status: Superseded (Apr 17 2003) (Accepted Aug 25 1998)
Units: Feet
Control Station: 9410660 Los Angeles, CA
T.M.: 0
Epoch: (/datum_options.html#NTDE) 1960-1978
Datum: NAVD88

Datum	Value	Description
MHHW (/datum_options.html#MHHW)	8.52	Mean Higher-High Water
MHW (/datum_options.html#MHW)	7.75	Mean High Water
MTL (/datum_options.html#MTL)	5.92	Mean Tide Level
MSL (/datum_options.html#MSL)	5.90	Mean Sea Level
DTL (/datum_options.html#DTL)	5.82	Mean Diurnal Tide Level

Datum	Value	Description
MLW (/datum_options.html#MLW)	4.09	Mean Low Water
MLLW (/datum_options.html#MLLW)	3.11	Mean Lower-Low Water
NAVD88 (/datum_options.html)		
STND (/datum_options.html#STND)	0.00	Station Datum
GT (/datum_options.html#GT)	5.41	Great Diurnal Range
MN (/datum_options.html#MN)	3.66	Mean Range of Tide
DHQ (/datum_options.html#DHQ)	0.77	Mean Diurnal High Water Inequality
DLQ (/datum_options.html#DLQ)	0.98	Mean Diurnal Low Water Inequality
HWI (/datum_options.html#HWI)	5.59	Greenwich High Water Interval (in hours)
LWI (/datum_options.html#LWI)	11.59	Greenwich Low Water Interval (in hours)
Max Tide (/datum_options.html#MAXTIDE)	10.79	Highest Observed Tide
Max Tide Date & Time (/datum_options.html#MAXTIDEDT)	12/13/2012 16:36	Highest Observed Tide Date & Time
Min Tide (/datum_options.html#MINTIDE)	0.27	Lowest Observed Tide
Min Tide Date & Time (/datum_options.html#MINTIDEDT)	12/17/1933 08:00	Lowest Observed Tide Date & Time
HAT (/datum_options.html#HAT)	10.33	Highest Astronomical Tide
HAT Date & Time	12/02/1990 16:24	HAT Date and Time
LAT (/datum_options.html#LAT)	1.10	Lowest Astronomical Tide
LAT Date & Time	01/01/1987 00:18	LAT Date and Time

Tidal Datum Analysis Periods
01/01/1974 - 12/31/1976
01/01/1978 - 12/31/1980

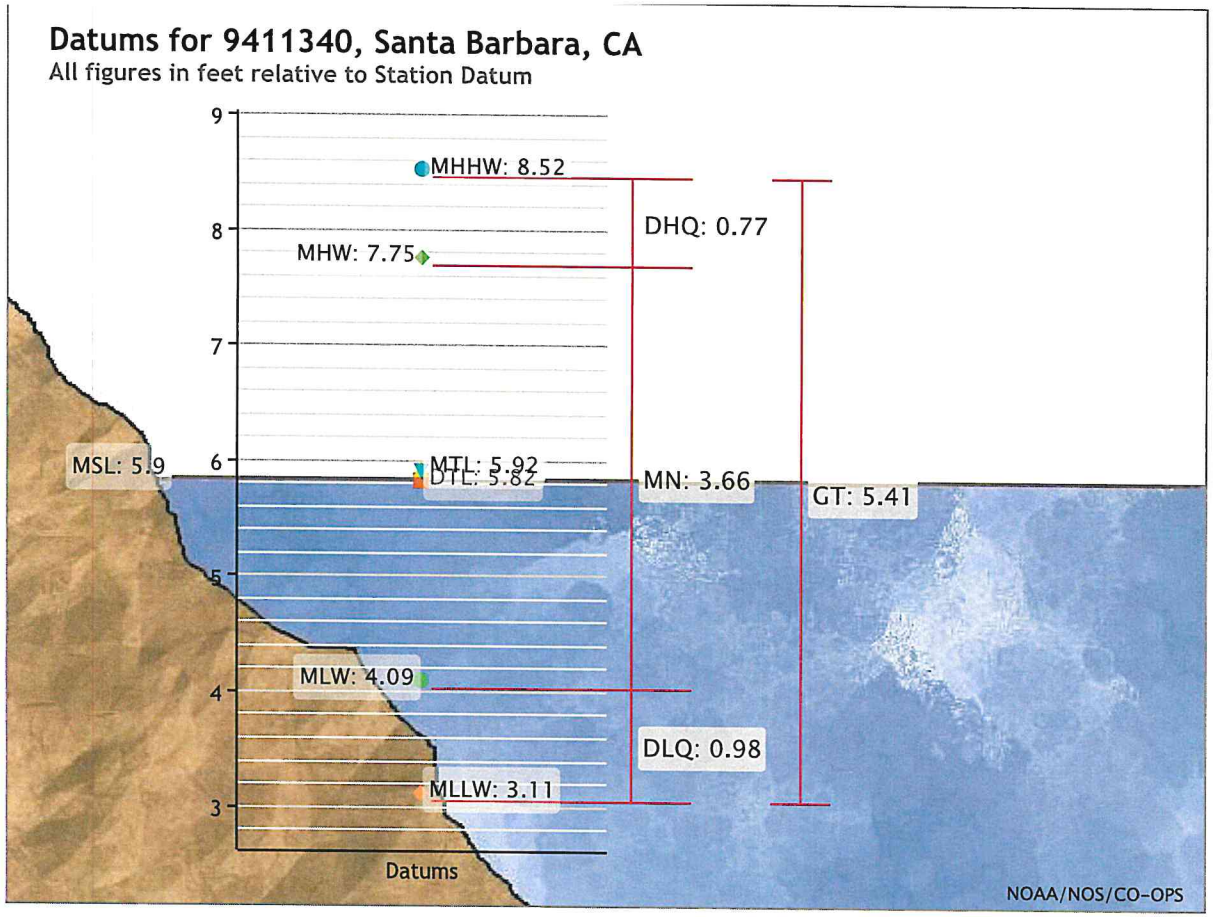

Showing datums for

9411340 Santa Barbara, CA

Datum

NAVD88

Data Units (•) Feet ( ) Meters

Epoch ( ) Present (1983-2001) (•) Superseded (1960-1978)

Submit

Show nearby stations

Products available at 9411340 Santa Barbara, CA

TIDES/WATER LEVELS

Water Levels (/waterlevels.html?id=9411340)

NOAA Tide Predictions (/noaatidepredictions.html?id=9411340)

Harmonic Constituents (/harcon.html?id=9411340)

Sea Level Trends (/sltrends/sltrends_station.shtml?id=9411340)

Datums (/datums.html?id=9411340)

Bench Mark Sheets (/benchmarks.html?id=9411340)

Extreme Water Levels

Reports (/reports.html?id=9411340)

METEOROLOGICAL/OTHER

Meteorological Observations (/met.html?id=9411340)

Water Temp/Conductivity

PORTS®

This station is not a member of PORTS®

OPERATIONAL FORECAST SYSTEMS

This station is not a member of OFS

INFORMATION

Station Home Page (/stationhome.html?id=9411340)

Data Inventory (/inventory.html?id=9411340)

Measurement Specifications (/measure.html)

Website Owner: Center for Operational Oceanographic Products and Services

National Oceanic and Atmospheric Administration (http://www.noaa.gov)
National Ocean Service (http://oceanservice.noaa.gov)
Privacy Policy (/privacy.html)
Disclaimer (/disclaimers.html)
Take Our Survey (/survey.html)
Freedom of Information Act (https://www.noaa.gov/foia-freedom-of-information-act)
Contact Us (/contact.html)

Datums for 9411340, Santa Barbara CA

NOTICE: All data values are relative to the NAVD88.

Elevations on NAVD88

Station: 9411340, Santa Barbara, CA
Status: Accepted (Oct 26 2020)
Units: Feet
Control Station: 9410840 Santa Monica, CA
T.M.: 0
Epoch: (/datum_options.html#NTDE) 1983-2001
Datum: NAVD88

Datum	Value	Description
MHHW (/datum_options.html#MHHW)	5.26	Mean Higher-High Water
MHW (/datum_options.html#MHW)	4.51	Mean High Water
MTL (/datum_options.html#MTL)	2.68	Mean Tide Level
MSL (/datum_options.html#MSL)	2.65	Mean Sea Level
DTL (/datum_options.html#DTL)	2.56	Mean Diurnal Tide Level

Datum	Value	Description
MLW (/datum_options.html#MLW)	0.84	Mean Low Water
MLLW (/datum_options.html#MLLW)	-0.13	Mean Lower-Low Water
NAVD88 (/datum_options.html)	0.00	North American Vertical Datum of 1988
STND (/datum_options.html#STND)	-3.27	Station Datum
GT (/datum_options.html#GT)	5.39	Great Diurnal Range
MN (/datum_options.html#MN)	3.66	Mean Range of Tide
DHQ (/datum_options.html#DHQ)	0.75	Mean Diurnal High Water Inequality
DLQ (/datum_options.html#DLQ)	0.98	Mean Diurnal Low Water Inequality
HWI (/datum_options.html#HWI)	5.53	Greenwich High Water Interval (in hours)
LWI (/datum_options.html#LWI)	11.59	Greenwich Low Water Interval (in hours)
Max Tide (/datum_options.html#MAXTIDE)	7.52	Highest Observed Tide
Max Tide Date & Time (/datum_options.html#MAXTIDEDT)	12/13/2012 16:36	Highest Observed Tide Date & Time
Min Tide (/datum_options.html#MINTIDE)	-3.00	Lowest Observed Tide
Min Tide Date & Time (/datum_options.html#MINTIDEDT)	12/17/1933 08:00	Lowest Observed Tide Date & Time
HAT (/datum_options.html#HAT)	7.08	Highest Astronomical Tide
HAT Date & Time	12/02/1990 16:24	HAT Date and Time
LAT (/datum_options.html#LAT)	-2.15	Lowest Astronomical Tide
LAT Date & Time	01/01/1987 00:18	LAT Date and Time

Tidal Datum Analysis Periods
01/01/1991 - 12/31/1997
11/01/2005 - 10/31/2007
04/01/2008 - 03/31/2010
06/01/2010 - 05/31/2019

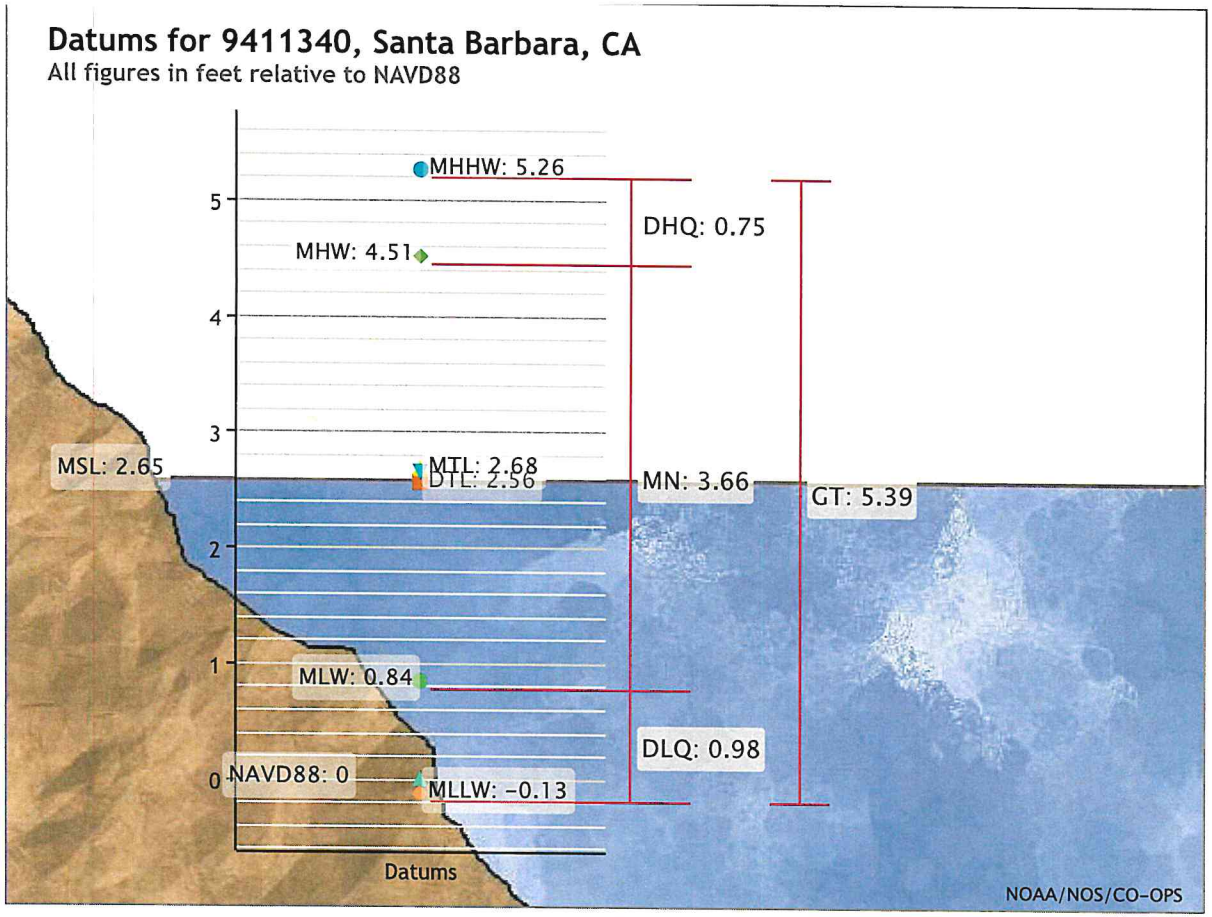

Showing datums for

9411340 Santa Barbara, CA

Datum

NAVD88

Data Units ◉ Feet
○ Meters

Epoch ◉ Present (1983-2001)
○ Superseded (1960-1978)

Submit

Show nearby stations

Products available at 9411340 Santa Barbara, CA

TIDES/WATER LEVELS

Water Levels (/waterlevels.html?id=9411340)

NOAA Tide Predictions (/noaatidepredictions.html?id=9411340)

Harmonic Constituents (/harcon.html?id=9411340)

Sea Level Trends (/sltrends/sltrends_station.shtml?id=9411340)

Datums (/datums.html?id=9411340)

Bench Mark Sheets (/benchmarks.html?id=9411340)

Extreme Water Levels

Reports (/reports.html?id=9411340)

METEOROLOGICAL/OTHER

Meteorological Observations (/met.html?id=9411340)

Water Temp/Conductivity

PORTS®

This station is not a member of PORTS®

OPERATIONAL FORECAST SYSTEMS

This station is not a member of OFS

INFORMATION

Station Home Page (/stationhome.html?id=9411340)

Data Inventory (/inventory.html?id=9411340)

Measurement Specifications (/measure.html)

Website Owner: Center for Operational Oceanographic Products and Services

National Oceanic and Atmospheric Administration (http://www.noaa.gov)
National Ocean Service (http://oceanservice.noaa.gov)
Privacy Policy (/privacy.html)
Disclaimer (/disclaimers.html)
Take Our Survey (/survey.html)
Freedom of Information Act (https://www.noaa.gov/foia-freedom-of-information-act)
Contact Us (/contact.html)

GEOPHYSICAL RESEARCH LETTERS, VOL. 0, NO. 0, PAGES 0-0, M 0, 2000

Tsunamis Within the Eastern Santa Barbara Channel

Jose C. Borrero, James F. Dolan, and Costas Emmanuel Synolakis

University of Southern California, Los Angeles CA, 90089-2531

Abstract. Several locally generated tsunamis have been reported in Southern California during the past 200 years, yet the hazard from locally generated tsunamis has received considerably little attention. We consider here tsunamis generated by coseismic displacements on the Channel Islands Thrust (CIT) system, as well as waves generated by slope failures along the walls of the Santa Barbara Channel. We find that purely tectonic sources could generate regional tsunamis with $\approx 2m$ runup, whereas combinations of tectonic sources and submarine mass movements could generate local runup as large as $\approx 15m$.

Introduction

Until the identification of the Cascadia subduction zone, the mitigation of locally generated tsunami hazards had received little attention, even for densely populated coastlines in the continental United States. Although historically tsunamis have caused enormous losses farfield, their long travel times allow for early warning. In contrast, locally generated tsunamis may have travel times as short as a few minutes. Furthermore, nearshore tsunamis may be enhanced by coseismic submarine mass failures. For example, the tsunami generated by the $M_w \approx 8.0$ Manzanillo, Mexico earthquake of 1995, hit the coast within $15min$ of the earthquake [*Borrero et al.*, 1995]; photos can be found at http://www.usc.edu/dept/tsunamis. Typical maximum runup values ranged from $2 - 4m$ – roughly as expected for the induced seafloor deformation. In contrast, the tsunami generated after the 1998 $M_w \approx 7.0$ Papua New Guinea earthquake produced runup in excess of $12m$ and caused major loss of life. *Kawata et al.*, [1999]. The cause of the extreme runup has been attributed to a large ($4km^3$) slump along the continental margin of Papua New Guinea [*Synolakis* in review].

These two and another ten tsunamis in the past decade struck nearby coastlines, but had little impact farfield, leading us to reassess the paradigm for tsunami hazards in southern California. McCulloch (1985) had earlier described the local hazard as 'moderate' with the potential for $2 - 4m$ runup heights. Following the 1992 Cape Mendocino earthquake, McCarthy et al. (1993) reassessed the risk to southern California from locally generated tsunamis as moderate to high. As Synolakis et al. (1997a) noted, these investigations were obtained without hydrodynamic modeling, using only earthquake magnitude–to–tsunami height relationships developed for Japan, which may not be appropriate for other tectonic settings. The region offshore Southern California has numerous possible tsunamigenic hazards, including submarine faults and mass failures on unstable basin slopes [*McCulloch*, 1985; *Vedder et al.*, 1986; *McCulloch et al.*, 1989]. Computational tools now exist *Synolakis et al.*, [1997b] to allow quantitative modeling of the inundation potential from locally generated events. We present here results from modeling tsunamis that could be triggered from faulting and submarine mass movements within the Santa Barbara Channel.

Paper number 1999GL000000.
0094-8276/00/1999GL000000$05.00

Regional Geologic Setting

Southern California lies astride a major transition between two tectonic provinces. The region to the south is dominated by northwest–trending, right–lateral strike-slip faults. The area to the north is characterized by west-trending mountain ranges–the Transverse Ranges–that have developed above west-trending reverse faults. Understanding of the thrust faults of the Transverse Ranges has increased dramatically over the past several decades, revealing the presence of several major reverse fault systems e.g. *Davis et al.*, [1989]; *Shaw and Suppe* [1994]; *Dolan et al.*, [1995].

The E–W Santa Barbara Channel forms the submerged western end of the Ventura basin *Vedder, et al.* [1969]. It is $\approx 130km$ long, extending from Point Conception in the west to the eastern end of Anacapa Island. The SB channel reaches a maximum depth of over $600m$ (fig. 1).

Several major active thrust fault systems, including the Channel Islands Thrust (CIT) of Shaw and Suppe (1994) lie offshore, beneath the Santa Barbara Channel. Potential coseismic deformation associated with this fault system represent a significant potential source for tsunami generation. Furthermore, the walls of the basin forming the channel are susceptible to submarine slope failures. At least two slope failures have been mapped in the central Santa Barbara Channel, one believed to have been seismically induced *Vedder et al.* [1986]; *McCulloch et al.* [1989]; *Edwards et al.*, [1993]. Recent studies reveal details of these two slope failures, additional failures along the northern wall of the channel, and several other possibly unstable regions *Greene and Maher,* [2000].

Historical Tsunamis and Earthquakes offshore Southern California

December 21, 1812 Santa Barbara. This one of the first reported large earthquakes in California appears to have generated a moderate-sized tsunami. The wave reportedly affected over $60km$ of the Santa Barbara coast *Toppozada et al.*, [1981]; *Lander et al.*, [1993]. This $M_w \approx 7.2$ earthquake caused extensive damage to the Spanish missions in the area. Historical sources report unusual ocean activity and high waves following the 12/21/1812 tremor *McCulloch* [1985]. Runup from this event is believed to have been as much as $4m$ at El Refugio, $40km$ west of Santa Barbara, and $\approx 2m$ in Santa Barbara and Ventura. Contemporary eyewitness accounts report that "the sea receded and rose like a high mountain", and "...it has been necessary for us to withdraw for now, more than half a league inland" *Toppozada et al.*, [1981]. Other accounts from survivors describe

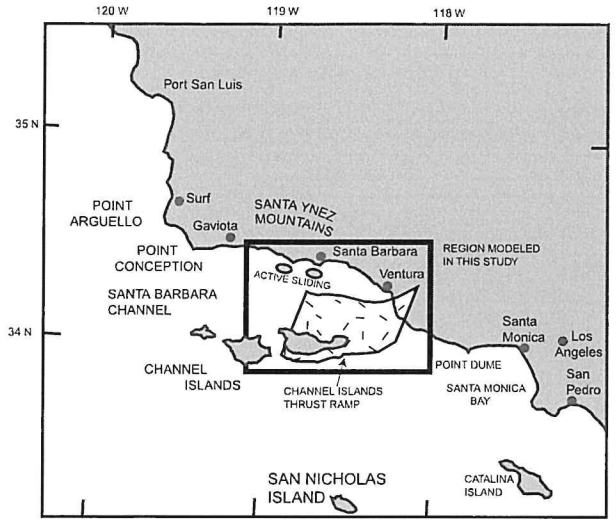

Figure 1. The southern California coast and locations mentioned in the text. The area within the box was the region used in numerical models. The hatchured area is the shape of the Channel Islands Thrust ramp as described by Shaw and Suppe (1994).

residents along the coast relocating their settlements further inland after being flooded by unusual waves. Lander et al. (1993) also report that this tsunami may have produced $4m$ runup in Kona, Hawaii.

November 4, 1927 Point Arguello-Lompoc. Even though outside our study region, the largest and best–observed locally generated tsunami on the entire west coast was triggered by the $M_s \approx 7.0$ November 4, 1927 Point Arguello-Lompoc earthquake northwest of Point Conception *Byerly* [1930]. The causative fault and exact location of this earthquake have been much debated, but the event is now believed to have occurred on an offshore thrust or oblique–reverse fault oriented parallel to the coast west of Point conception *Helmberger et al.*, [1992]. The tsunami generated by this event was observed in several locations along central California coast, and even reached Hawaii. A $2m$ wave was observed in Surf just north of Point Arguello, while at Port San Luis, a reported $2m$ recession was followed by a similar rise *Byerly* [1930]; *Lander et al.*, [1993]. Newspaper accounts from San Pedro, California south of Los Angeles describe an "exceptionally high tide" $1hr$ after the event but "no damage". Simulations of this tsunami match contemporary observations and helped relocate the source *Satake and Somerville* [1992].

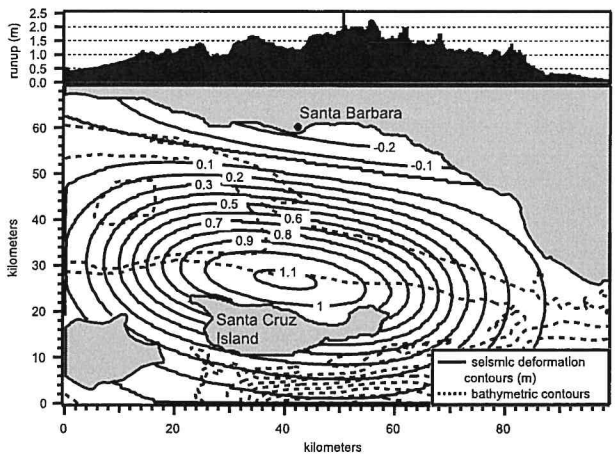

Figure 2. Co-seismic deformation contours (solid lines) in meters from a complete rupture of the Channel Islands Thrust Fault. The computed tsunami is represented as the vertical black bars above the map.

Seismic Tsunami Sources

Channel Islands Thrust (CIT). The Channel Islands Thrust is an N–dipping blind thrust fault that is responsible for uplift of the Channel Islands S. of the Santa Barbara coast (fault plane shown as the stippled region on fig. 1) *Shaw and Suppe* [1994]. These islands represent the crest of the predominantly submarine, southernmost Transverse Ranges. Shaw and Suppe's (1994) balanced cross–section models indicate that the CIT dips gently (23°) N. from a depth of about $7km$ beneath the S. edge of Santa Cruz island, to a depth of $\approx 17km$ beneath the Santa Barbara coast. The main thrust ramp that they modeled extends along strike for $40km$ from east of Santa Cruz Island to its west end, with a total fault plane area of $1900km^2$. Shaw and Suppe (1994) used these fault parameters to estimate a maximum surface–wave magnitude $M_s \approx 7.2 - 7.3$ and slip estimates of comparable earthquakes to estimate $\approx 2m$ of average coseismic displacement, for a complete rupture. Regressions by Wells and Coppersmith (1994) relating fault plane area, eq. magnitude, and average slip yield similar values of $M_w \approx 7.3$ and average slip of $\approx 2.8m$. Regressions in which only southern California earthquakes are considered *Dolan et al.*, [1995] yield larger estimates of maximum magnitude of $M_w \approx 7.4$, and average slip/event $3.5 - 4m$.

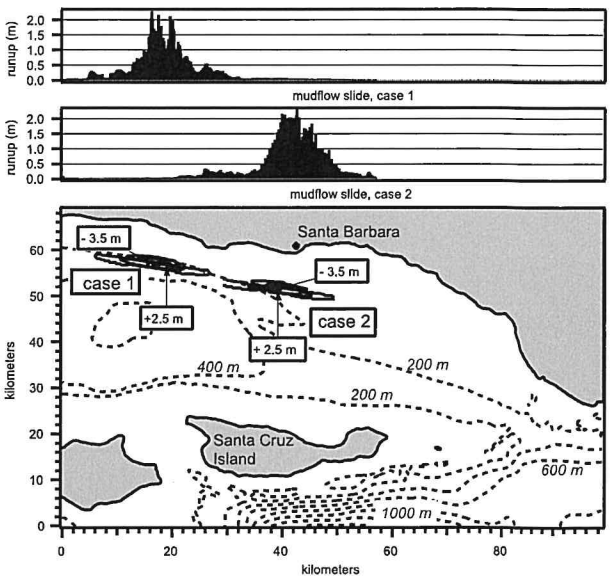

Figure 3. Tsunami runup produdced by slide 1, modeled after seismically induced mudflow described by Edwards and Lee (1993). Two cases are shown with the initial condition placed in different locations off of the coast. Note how the runup pattern stays basically the same, and is shifted along the coast.

Although the main N–dipping CIT ramp does not reach the seafloor, its large size and the possibility of large slip per event suggests that it has the potential to produce $\approx 2m$ vertical uplift of the seafloor.

The CIT is the master thrust fault of a system of blind and surficial thrust faults that extend along the Santa Barbara coast. Several of these active faults, including the Pitas Point Thrust and the North Channel Slope fault, they could also generate significant vertical uplift of the seafloor, but they are not modeled in this study.

Other Tsunami Sources

In recent decades, tsunami research has focused on waves directly generated by coseismic uplift of the seafloor induced by fault slip. Motivated by the 1998 Papua New Guinea *Kawata et al.,* [1999] and 1999 Vanuatu [*Synolakis,* in prep]. tsunamis enhanced by underwater mass movements, we model three hypothetical offshore slides to assess their possible impact. We note however that detailed marine geologic investigations of offshore slope stability and evidence of past submarine slope failures are urgently needed to determine the true tsunamigenic potential of offshore slides in Southern California.

We first consider a hypothetical tsunami generated by a small, $0.2km^3$ mudflow *Watts,* pers. comm., 1998, as per marine geophysical data offshore of Gaviota, W. of Santa Barbara *Edwards et al.,* [1993]. We then consider a hypothetical tsunami generated by a much larger $4km^3$ slide, where we use the offshore slide believed to be responsible for generating the 1998 PNG tsunami, as per [*Synolakis* in review]. These two initial conditions are used in order to provide a possible range of runup values that could be expected from a submarine mass movement within the Santa Barbara Channel, with the mudflow case and the PNG case (slide2) as plausible lower and upper bounds, respectively.

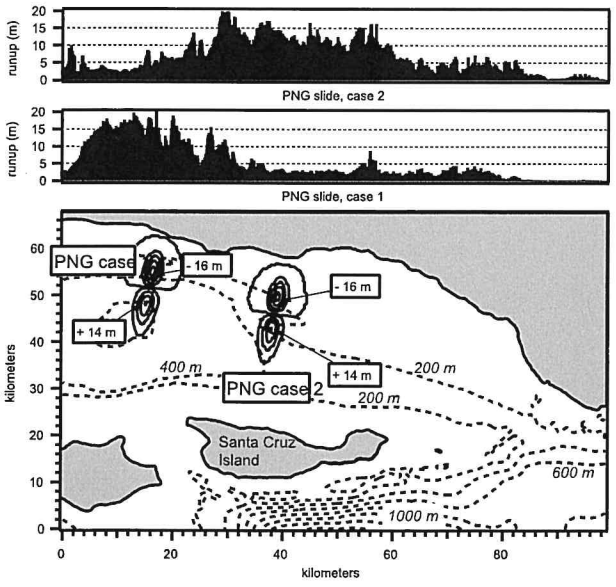

Figure 4. Tsunami runup produced by slide 2, modeled after a larger, thicker mass faliure, simmilar to the one believed to have caused the 1998 Papua New Guinea Tsunami. Again, two location scenarios are shown.

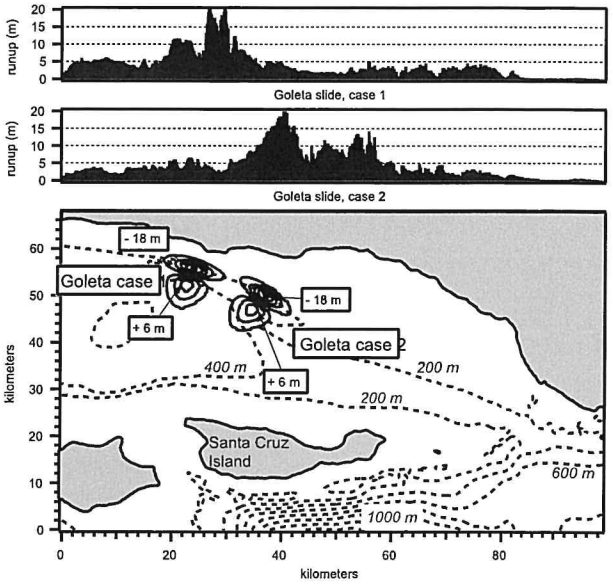

Figure 5. Tsunami runup produced by slide 3, modeled after a slide identified offshore of Goleta, California by Greene and Maher 2000. Again, two location scenarios are shown.

The slide parameters that most affect tsunami generation are not yet well established, and the prediction of waves generated by future mass movements remains a formidable undertaking *Synolakis et al.,* [1997b]. Although the $4km^3$ Papua New Guinea slump is larger than any slides that have thus far been observed offshore southern California, its mean initiation depth at $\approx 1200m$ is much deeper than the shallower water depths $100-500m$ in the Santa Barbara Channel, implying much more efficient wave generation, and compensating for the smaller volumes. We checked this conjecture by modeling the recently identified Goleta slide of *Greene and Maher,* [2000], per their preliminary parameters provided in http://www.mbari.org. Other slope failures have been identified offshore southern California *McCulloch* [1985]; *Edwards et al.,* [1993], and detailed surveys to identify other failure features are currently underway *Greene and Maher,* [2000].

Discussion

Given a fault solution, the prevailing paradigm in tsunami inundation modeling uses elastic dislocation theory to estimate the seafloor deformation, which is assumed to be instantaneous so as to allow use of the shallow water (SW) wave equations without forcing terms. Here, we used VTCS–3 (a.k.a. MOST), one of the two existing $2+1$ nonlinear SW codes, validated with laboratory and field data *Yeh et al.,* [1996]. MOST predicts wave evolution over irregular bathymetries by utilizing a variable grid that allows a consistent number of grid nodes per wavelength. Inundation is calculated without using artificial viscosity or friction terms *Titov and Synolakis* [1998].

We used a variety of maps and sources to develop a $250m$ computational grid. Onshore topography was verified with field surveys in selected locales along the Santa Barbara coast. Whereas the location of the seismic sources are constrained by geology, the location of a potential landslide is

more variable. We therefore performed multiple runs in different suspicious locales off the coast.

As shown in figs. 2 and 3, the CIT and mudflow slide, both have the potential to generate $2m$ runup along the coast. For the CIT, the maximum runup appears near the center of the source and remains fairly constant until it drops off outside of the deformed region. The mudflow slide could potentially augment the runup of a seismic source *see Geist* [2000]; if the slide occurs within the zone of tectonic uplift, maximum runup would be approximately the sum of the tectonic–and slide–induced waves. If , as in fig. 2, the slide lies outside of the region of tectonic uplift or occurs a significant time after the earthquake induced wave, it is manifested as a narrow runup peak.

The simulation of the PNG–style slide in fig. 4 generates runup in excess of $15m$, similar to the simulations and observed values in Papua New Guinea. We observe an area of runup greater than $10m$ over a $20km$ stretch of coast, with maximum runup of nearly $20m$. This zone is superimposed on a much broader, $\approx 100km$–long area of $2-4m$ runup. Figure 5 shows the runup values for a wave generated by the Goleta slide, *Greene and Maher,* [2000]. The distribution is different, but extreme values in excess of $15m$ are similar with the PNG–style slide. Extreme runup of this size anywhere along populated shores would be devastating. However, uncertainties in the calculations of slide evolution, directivity and localization suggest using the runup distributions' more representative values of $10-15m$ as a guide for emergency planning.

These are the first quantitative hydrodynamic calculations of locally generated tsunamis offshore southern California. This type of analysis is important for realistic tsunami hazard assessment along the densely populated coastlines, and has been the basis for generating tsunami hazard maps throughout the western United States. Future studies of locally generated tsunamis in Southern California depend on more accurate mapping and dating of submarine slope failures, better combined bathymetry and topography data, and improved hydrodynamic models of wave generation from landslides and seismic sources.

Acknowledgments. We gratefully acknowledge support from the Federal Emergency Management Agency, the Governor's Office of Emergency Services of California, the State Lands Commission, and the Seismic Safety Commission. We would also like to thank Eddie Bernard, Frank Gonzalez and Vasily Titov of the Tsunami Program of NOAA's Pacific Marine Environmental Laboratory for valuable input.

References

Borrero J.C., M. Ortiz, V.V. Titov, and C.E. Synolakis, Field survey of Mexican tsunami produces new data, unusual photos, *Eos Trans. AGU, 78, # 8,* 85, 87-88, 1995.

Byerly, P.,The California Earthquake of November 4, 1927, *Bull. Seismol. Soc. Am., 20,* 53-66, 1930.

Davis, T., J., Namson, and R. Yerkes, A Cross Section of the LA Area: Seismically Active Fold and Thrust Belt, *J. Geophys. Res., 94,* No. B7 9644 -9664, 1989.

Dolan, J. F. et al., Prospects for larger or more frequent earthquakes in the Los Angeles Metropolitan region, *Science 267,* 199–205, 1995.

Edwards, B.D., H.J. Lee, and M.F. Field, Seismically induced mudflow in Santa Barbara Basin, in *USGS Bull., 2002,* 167–175, 1993.

Geist, E., Origin of 17 July 1998 Papua New Guinea Tsunami: Earthquake or Landslide? *Seismological Review Letters 71 #3,* 344 - 351, 2000.

Greene, G., and N. Maher, Slope Instability and the Potential for Tsunami Generating Landslides, NSF Workshop on the Prediction of Underwater Landslide and Slump Occurrence of Southern California, Los Angeles, CA, 2000.

Helmberger, D.V., P.G. Somerville, and E. Garnero, The location and source parameters of the Lompoc, California Earthquake of 4 November 1927. *Bull. Seismol. Soc. Am., 82, # 4,* 1678-1709, 1992.

Kawata, Y., B. Benson, J.C. Borrero, J.L. Borrero, H.L. Davies, W.P. deLange, F. Imamura, H. Letz, J. Nott, and C.E. Synolakis, Tsunami in Papua New Guinea was as Intense as First Thought, *Eos Trans. AGU, 80, # 9,* 101, 104-105, 1999.

Lander, J., P.Lockridge, and M. Kozuch (Eds.), *Tsunamis Affecting the West Coast of the United States,* 242 pp., U.S. Department of Commerce, NOAA, 1993.

McCarthy, R.J., Bernard, E.N., and Legg, M.R., Cape Mendocino Earthquake: A wake Local Tsunami Wakeup Call?, paper presented at the Symposium on Coastal and Ocean Management, New Orleans, LA, July 19-23 1993.

McCulloch, D., Evaluating tsunami potential, in *USGS Prof. Paper 1360* pp. 375–414, 1985.

McCulloch, D.S., Geologic map of the south-central California continental margin (Map No. 4A, Scale 1:250,000), CDMG, 1989.

Satake, K. and P. Somerville, Location and Size of the 1927 Lompoc, California Earthquake from Tsunami Data, *Bull. Seismol. Soc. Am., 82* 1710-1725, 1992.

Shaw, J. and J. Suppe, Active faulting and growth folding in the eastern Santa Barbara Channel, California, *Geol. Soci. of Am. 106,* 607-626, 1994.

Synolakis, C.E., Liu, P.L.-F, Carrier, G., Yeh, H.H., Tsunamigenic Seafloor Deformations *Science 278,* 598-600, 1997.

Synolakis, C.E., D. McCarthy, V. Titov, J. Borrero, Evaluating the Tsunami Risk in Southern California, paper presented at the California and the World Oceans '97 conference, San Diego, CA 3/24-27/97.

Synolakis, C.E., Bardet, J-P., Borrero, J.C., Davies, H., Grilli, S., Okal, E., Silver, E., Sweet, S., Tappin, D., Watts, P., The Slump origin of the 1998 Papua New Guinea Tsunami, *in review,* 2001.

Synolakis, C.E., Moore, A., Kanoglu, U., Ruscher, C., Field Survey of 1999 Vanuatu Tsunami, *in preparation.*

Titov, V. and C., Synolakis, Numerical modeling of tidal wave runup, *Journal of Waterway, Port, Coastal and Ocean Engineering 124,* 157-171, 1998.

Toppozada, T., C. Real, and D. Parke, Preparation of isoseismal maps and summaries of of pre– 1900 California Eqs., *CDMG # 81-11SAC,* p. 34, 136–140, 1981.

Vedder, J.G., H.C. Wagner, J.E. Schoellhamer, Geologic Framework of the Santa Barbara Channel Region, in *USGS Prof. Paper 679–D,* pp. 1–11, 1969.

Vedder, J.G., Greene, H.G., Clark, S.H., and Kennedy, M.P., Geologic map of the mid–S. California continental margin (Map No. 2A Scale 1:250,000), CDMG, 1986.

Watts, P., Wavemaker curves for tsunami generated by underwater landslides, *J. Waterway, Port, Coastal and Ocean Engineering 124 # ,3,* 127–137, 1998.

Watts, P., Personal Communications, 1998.

Wells, D. and K., Coppersmith, New empirical relationship among magnitude,rupture length, rupture width, rupture area and surface displacement, *Bull. Seismol. Soc. Am., 84 # ,4,* 974–1002, 1994.

Yeh, H., P. Liu, and C.E. Synolakis (Eds.), *Long Wave Runup Models,* 403 pp., World Scientific, New Jersey, 1996.

J.C. Borrero, J. Dolan, C.E. Synolakis, University of Southern California, Los Angeles, California 90089–2531 (e-mail: jborrero@usc.edu, dolan@usc.edu, costas@usc.edu)

(Received July 3, 2000; revised October 24, 2000; accepted October 31, 2000.)

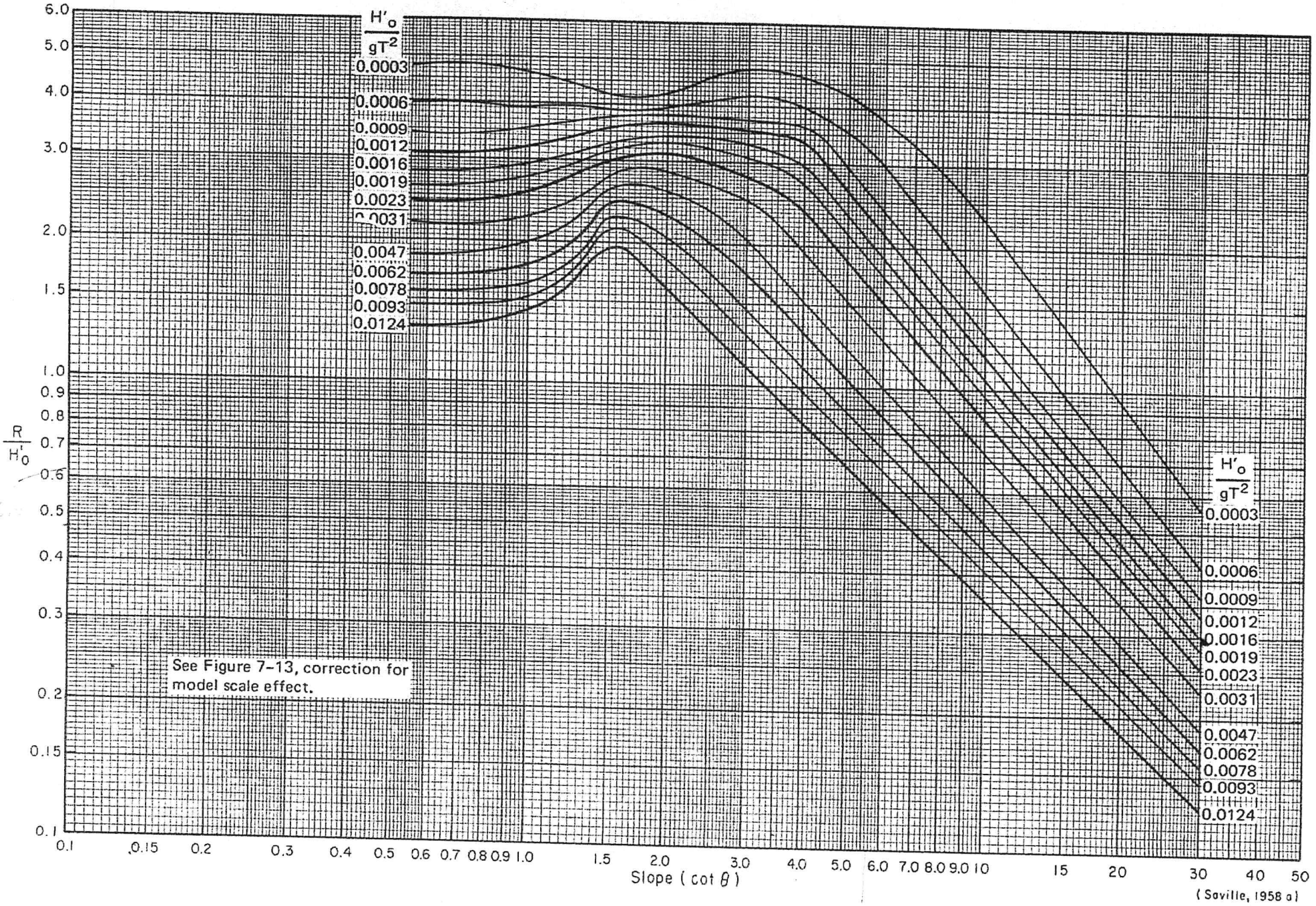

Figure 7-11. Wave runup on smooth, impermeable slopes when $d_s/H'_o \approx 2.0$.